Book of Tutorials and Abstracts

European
Microbeam Analysis Society

University of BRISTOL

Mineralogical Society

EMAS 2018

13th EMAS Regional Workshop

MICROBEAM ANALYSIS IN THE EARTH SCIENCES

4 - 7 September 2018

University of Bristol, Wills Hall, Bristol, Great Britain

Organised in collaboration with:
Mineralogical Society of Great Britain and Ireland
and
University of Bristol

THE USE OF RAMAN AND MICRO-ATR (FTIR) SPECTROSCOPIES TO MEASURE VOLATILE SPECIES IN SILICATE GLASSES

R.A. Brooker and D. Di Genova

University of Bristol, School of Earth Sciences
Wills Memorial Building, Queens Road, Bristol BS8 1RJ, Great Britain
e-mail: richard.brooker@bristol.ac.uk

ABSTRACT

Increasingly, Raman and more recently micro-ATR (attenuated total reflectance) are being used to analyse water and carbon dioxide in geological glasses where thin wafer sample preparation for more traditional transmission IR proves difficult. We review recently published (and 'in progress') practical developments in this field for measurement of both water and carbon dioxide species dissolved in geologically relevant silicate glasses. For Raman advance have been made in understanding the complexity of the silicate peaks used to standardise the volatiles concentrations and for ATR we extend the compositional range covered for water and new data for CO_2.

1. INTRODUCTION

FTIR microscopy in transmission mode has traditionally been the main technique for quantitative analysis of water and CO_2 in geological silicate glasses, for both natural and experimental samples. Historically, IR was conducted on powdered glass diluted in pressed KBr pellets, but the accuracy of this method was always highly dependent on homogeneous mixing of very precisely known quantities of sample and in the case of water measurement, the total exclusion of absorbed moisture on the very high surface area of the powers involved. This method also requires large samples and special information is lost compared to later micro techniques. Reflectance microIR of a single highly polished surface has also been tested (see [1]), but the signal is dominated by the actual surface, rather than the body of the sample and interpretation of the spectra is not straightforward. Hence transmission IR through a double polished wafer became the most reliable method in many volatile studies with the transmission spectra converted to absorbance values for quantitative purposes [2-5]. The major drawback to this micro technique has been the requirement for thin parallel sided wafers to allow transmission through the sample (Fig. 1B). In practical terms for bench top spectrometers the sample must be thin enough to ensure the relevant volatile absorbance peaks are 'on scale' (not so many bonds that they are fully absorbed) and a beam size of at least 30 μm must be able to pass 'uninterrupted' through the sample. This leads to several competing factors for the analyst to consider. The practical one is the sample preparation, which is easy if a large amount of glass is available and millimetre sized wafers of 50 - 500 μm thickness can be prepared. In this case transmission IR can be one of the most accurate and sensitive techniques for measuring water (H_2O and OH) and carbon dioxide (molecular CO_2 and carbonate) species in glasses, down to the 10s of ppm level. However, in many natural and experimentally produced samples, the size of quenched glass inclusions or melt pockets between solid phases is too small in diameter or the solid phase distribution in 3D require unreasonably thin wafer preparation to find a clear, uninterrupted path through the glass. As a result, the demand has grown for 'one-sided' analytical techniques where a glass surface is exposed and polished, but a wafer is not required and the depth of penetration is minimal. Although ion probe analysis (SIMS) with a 15 - 30 μm beam has served many excellent studies to this end [6-8], this technique is expensive and access is very limited. This has led to the development of Raman [9-13] and ATR microFTIR [14] spectroscopies in an attempt to provide a practical and accessible solution to this problem.

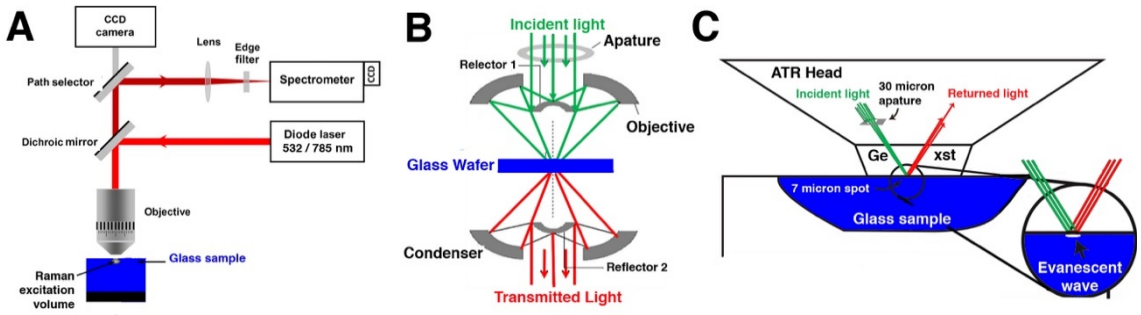

Figure 1. A schematic illustration of A) Raman, B) Transmission IR, and C) ATR techniques showing double polished wafer requirement for transmission. Note that the analysis area with ATR is 0.3 - 0.25 time smaller than the minimum 30 µm for transmission IR.

In vibrational terms, Raman and IR can be very complementary (see [15]). Some vibrational modes respond more strongly in one method than the other which can help identify structural information [16, 17]. As illustrated in Fig. 1, Raman generally requires no sample preparation (although a polished surface is desirable) and can focussed down to a 1 µm beam resolution. However, florescence and other problems with background fitting, silicate peak standardisation and the presence of nanolites do need to be addressed particularly for iron-bearing glasses. To avoid the difficulties associated with transmission, attenuated total reflectance (ATR) techniques have been developed, which uses an evanescent wave to penetrate into the surface of a sample. This effectively has a very short path length equivalent to a sample thinned to a few µm, but with only a single, polished surface required. There is also the potential for increased spatial resolution with ATR. To be fully quantitative for volatile measurement, both techniques require some specific calibration related to the bulk composition of the silicate glass.

As shown in Fig. 2 dissolved water and carbon dioxide can form several species in a melt depending on how these volatiles react with the silicate melt structure. For water, (Fig. 2A) hydroxyl O-H species prevail at low concentrations, but molecular H_2O increases to become more dominant at higher concentrations (e.g., [19]). For carbon dioxide (Figs. 2C to 2E), molecular CO_2 species are found in highly polymerised (high SiO_2) compositions, but CO_3^{2-} carbonate species dominate depolymerised or more cation-rich compositions [3, 4, 16, 19]. The vibrational species commonly used for quantifying total water are the O-H stretching vibrations at 3,500 cm^{-1}, as this has contribution from the O-H bond in hydroxyl and well as the O-H stretch within the H_2O molecules. As illustrated in Figs 2A and 2B, it is both IR and Raman active (e.g., [2, 20]). In transmission spectroscopy, this band at 3,500 cm^{-1} can be difficult to get 'on scale' for high water concentrations, requiring wafer preparation down to < 50 µm as total water approaches 4 wt%. This requires significant preparation skill and measuring the thickness accurately also become a major source of error in quantification. Fortunately for transmission spectroscopy, there are smaller bands (overtones, see Fig. 2A) that can be used, allowing much thicker wafers to be utilised assuming the sample is suitable. As Raman is relatively less sensitive and always 'on scale' (unless too much signal is accumulated) the 3,500 cm^{-1} peak is ideal for water quantification. For ATR, the effective

penetration depth (or beam path length) is frequency dependant but at 3,500 cm^{-1} is equivalent to thinning a sample to about 1 μm, so even 10 wt% water will easily be 'on scale' and the problem become one of sensitivity as low intensity peaks can be lost in background noise.

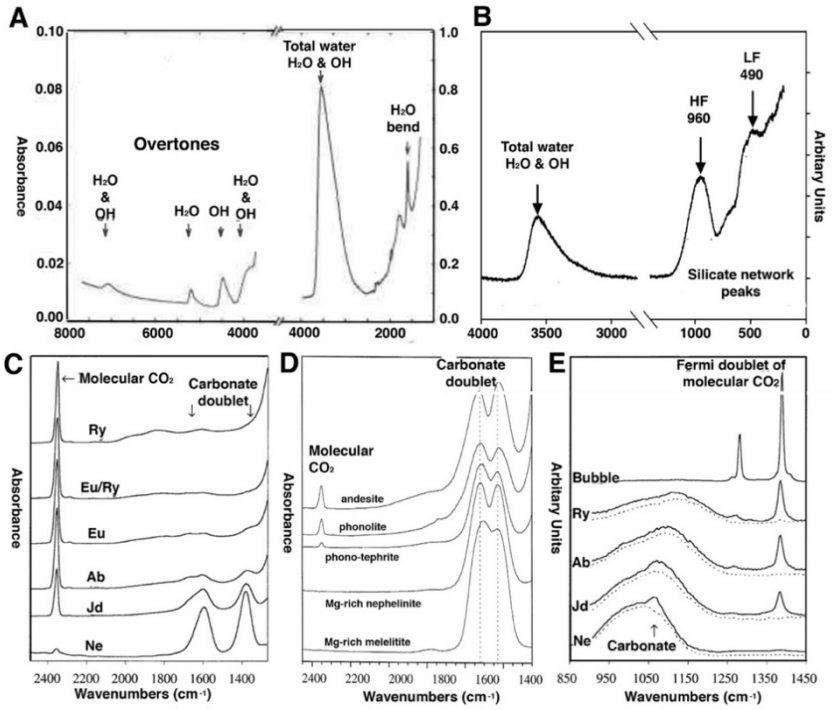

Figure 2. Transmission IR and Raman spectra for water (A and B) and carbon dioxide (C to E) species dissolved in silicate glasses (C to E). A shows the transmission IR spectra for a 50 μm wafer of rhyolite with ~ 1.24 wt% water [2]. Both OH and H_2O species are present and contribute to the large peak at 3,500 cm^{-1}. The much smaller overtones are also show (note the 10x expanded scale for these). B shows the Raman spectra of a basanitic glass with 4.96 wt% water [11] with the same 3,500 cm^{-1} total water band as in A. Also shown are the silicate peaks which form low (LF) and high (HF) frequency groups. C shows the transmission IR spectra are shown for glasses along the $NaAlO_2$-SiO_2 join [16] with a swap from molecular CO_2 to carbonate as more $NaAlO_2$ is added. A similar progression with depolymerisation is also shown for natural rock compositions in D (from [17]). E shows the Raman spectra for selected samples in C and the dashed line is for a CO_2 free sample. The spectrum for a CO_2 gas bubble is also shown to illustrate the Fermi doublet [16].

For carbon dioxide, molecular CO_2 is the only species dissolved in more silicic glasses such as rhyolites. As compositions become less silicic, carbonate also appears. Both species might be present in an 'intermediate' andesite (Fig. 2D), but eventually carbonate becomes the only species as more metal cations are added and silica falls to the levels in basalt. Molecular CO_2 has an IR active asymmetric stretch at 2,350 cm^{-1} (Fig. 2b) and in theory a Raman active symmetric stretch peak at 1,330 cm^{-1}, although this is split into a 'fermi doublet' due to interaction with an IR active peak (e.g., [16]). The most useful IR active carbonate peak in the asymmetric stretch at ~1,415 cm^{-1}

which splits into a doublet (Figs 2C and 2D) related to the way the carbonate unit is distorted in the melt structure [17]. The main Raman active carbonate peak is for symmetric stretching at ~1,060 cm^{-1}. Unfortunately, this band is at the same position as the main silicate (or aluminosilicate) symmetric stretching peaks (Fig. 2E), so is difficult to see at low concentrations and requires some fitting to extract an independent intensity [13]. For transmission IR, a molecular CO_2 peak at 2,350 cm^{-1} representing only 0.7 wt% carbon dioxide would require wafers < 50 μm but at this frequency the ATR the penetration depth (equivalent wafer thickness) is only 2 μm. For either of the carbonate doublet peaks at 1,400 - 1,500 cm^{-1}, a 50 μm wafer could in theory cope with up to 1.75 wt% CO_2 but these can sit on the tail of the aluminosilicate peaks at ~1,000 cm^{-1} (see Fig. 2b), which can 'lift' them towards saturation, particularly for the low frequency side of the doublet and in high silica samples. For ATR, the depth of penetration at these frequencies is around 3 μm.

As previously discussed, transmission IR requires spectra to be taken through the sample then by comparison with a sample free background, the amount of absorbance can be calculated for any particular peak representing a vibrational frequency. This utilises the Beer-Lambert approximation to give a concentration where the peak intensity * the molecular weight is divided by the density * thickness, the thickness being the controllable variable. This value has to then be converted by a calibration factor called the extinction coefficient which is specific to that glass composition and must be determined by some other means (usually measuring similar samples with the volatile concentration determined by bulk analysis). For Raman, the absolute peak intensities themselves are arbitrary (they just increase as data is collected) so methods have been developed to ratio these to the silicate peak heights as shown in Fig. 3. As this study will show, it is this comparison with the silicate structure than is one of the major complications with this technique.

For ATR, the spectra are effectively taken as if in transmission mode and converted to an absorbance spectra (by also taking a sample free background), but the effective 'thickness' is no longer a controlled variable and not only varies with frequency but also the refractive index of the glass (density). As a result, some compositional calibration is required as will be shown illustrated in this study.

2. METHODS

2.1. Raman baseline subtraction and ratio to the silicate peaks

Many studies have illustrated that spectra contribution between ~3,000 and 3,800 cm^{-1} related to the vibration of both OH^- species and molecular water has an intensity and area positively correlate with the water content dissolved in the glass. But as Raman spectra have arbitrary units of intensity (they just increase with collection time, scan accumulation or laser power) the basic principle is to measure the silicate and water peaks and use the ratio to determine the water content

(e.g., [9-11, 21,22]) and compare with a known standards of similar compositions (external calibration)) or try to develop modes that cover all compositions (internal calibration). This requires the fitting of a baseline to remove spurious background features (that can vary between acquisitions on the same spectrometer on the same sample) and then measurement of the remaining peak areas as shown in Fig. 3.

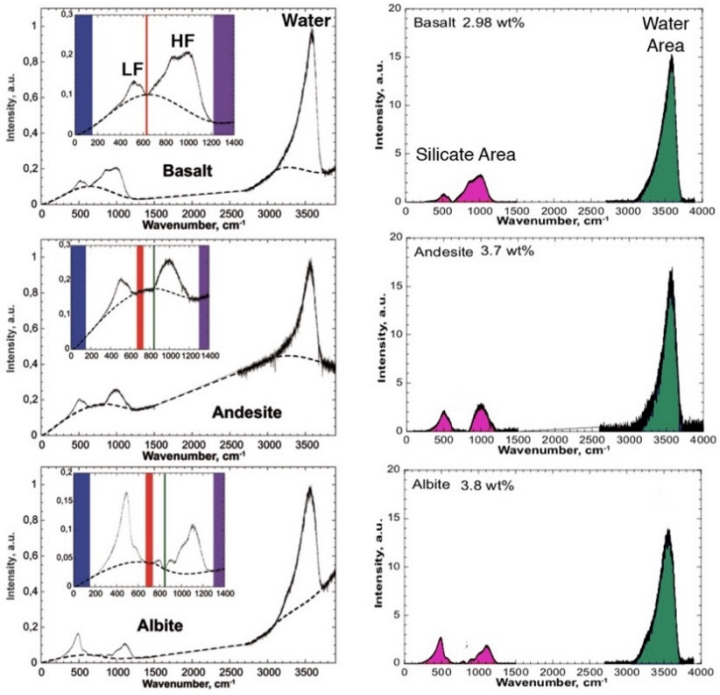

Figure 3. This illustrates the principle of using the ratio of the silicate peaks to the water peaks to quantify the water concentration. Some workers have used the higher frequency peaks, some the lower, or both. The fitting of the baseline is obviously crucial to this process and one particular example shown here in A, with common positions use to estimate where the dashed background should touch the spectra. Although the silicate peaks show different shapes and LF to HF ratios, it has been suggested that the sum of the two, relative to the water peak area might be considered constant, at least for a limited range of compositions. Modified from [12].

2.2. Raman Peak fitting for CO_2

A similar process to the ratio method for water can be used for carbonate, but the individual peaks must be fitted in the HF envelope to extract the carbonate peak area. A full account of this method has been given in Morizet *et al.* [13] and is not discussed further, but is shown in Fig. 4 for completeness.

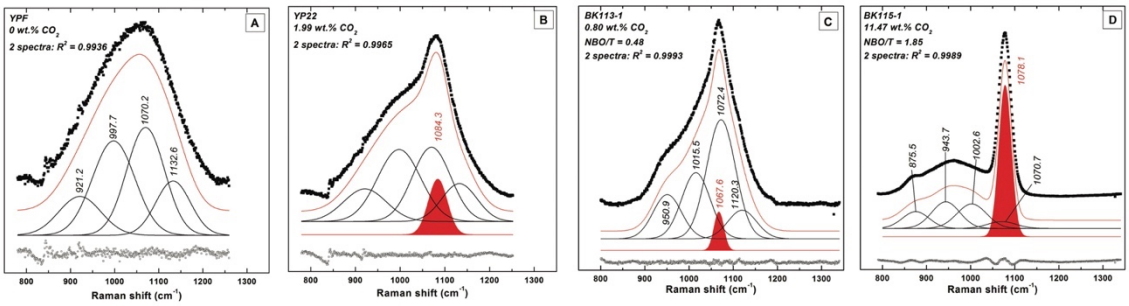

Figure 4. Raman spectra of glasses showing the carbonate symmetric stretching peak (in red) amongst the various peaks representing the aluminosilicate structure. In A and B represent the same composition with no CO_2 and ~2 wt% respectively, but C is a very different composition with different aluminosilicate structures, initially giving the false impression of higher CO_2 content than C until the fitting is completed. D is a more similar structure to A and B, but with far more CO_2. Adapted from Morizet *et al.* [13].

2.3. Sample preparation for ATR

Raman requires little preparation, although a flat polished surface is desirable for constant focussing, etc. However, the ATR principle requires the sample surface to be in intimate contact with the ATR crystal (usually germanium or diamond; see Fig. 1C). As the incoming beam is reflected off the lower crystal surface, an evanescent wave penetrates the sample to some depth. This requires some precise control and matching related to the refractive index of the crystal used. Any air (or other material with a different refractive index) that intervenes will stop the evanescent wave from penetrating. Intimate contact requires a well-polished flat surface and some pressure to be applied to force the crystal into the sample, ensuring complete contact. This also requires the sample surface to be parallel to the crystal surface. In practical terms it usually helps if the sample can self-level to meet the crystal. Glass mounted in a slightly plastic medium (such as resin) works well and if a resin block is use, some soft material beneath also helps with alignment (double-sided sticky tape is ideal). Delicate samples such as thin glass wafers need a balance between rotational adjustment and support against breakage as the ATM pressure is increased. Failure to exclude air will result in no spectrum, but partial contact can give erroneous results as shown in Fig. 5.

3. RECENT DEVELOPMENTS AND NEW RESULTS

Although general principles are well established for quantifying water by Raman, these are highly dependent on the fitting of backgrounds and determining the way the silicate peak areas relate to water for different compositions, oxidation state of the Fe and the presence of nanolites. We review the recent developments in this area. For ATR there appears to be a more simple calibration method dependant only on the density (or refractive index) of the glass, which we test for an extended compositional range. We present new data for analysing carbonate by ATR which also highlights the important of glass density.

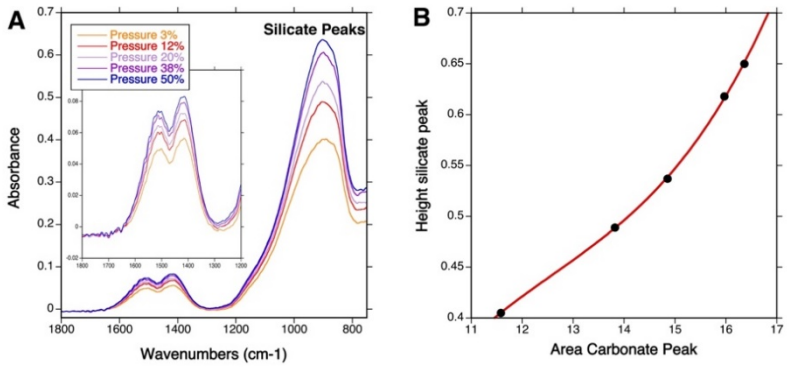

Figure 5. This illustrates a common problem when a sample surface is not in perfect contact with the ATR crystal or the polish is not of high quality. This allows air between some area of the crystal tip and the sample. In most cases there is no signal all, but even an apparent spectrum can give erroneous intensities. It tempting to assume all peaks are affected to the same extent and use the silicate peak to rescale the spectra, but as shown in B, this is not a linear relationship due to each frequency being affected to differing degrees.

3.1. Variation in the Raman silicate envelope

Figures 6A and 6B shows baseline-corrected Raman spectra of anhydrous rhyolite, andesite, and basanite glasses from Mercier *et al.* [11]. The chemical composition of glasses in the Mercier study spans a range of SiO_2 (76.29 - 41.14) and FeO (11.99 - 1.36) content which covers the majority of magma erupted on Earth. Two main bands can be observed in Fig. 6A between ~800 and ~1,300 cm^{-1} and from ~200 to ~600 cm^{-1} respectively the so called high and low frequency envelopes (HF and LF in Fig. 3). These Raman bands arise from the spectroscopic response of the glass structure [23-25]. The first region (~200 and ~600 cm^{-1}) arise from the vibration of bridging oxygens bonded to tetrahedra that, in geological silicate systems, are coordinate to Si^{4+}, Al^{4+}, and Fe^{3+} cations (T). The second region (~800 to ~1,300 cm^{-1}) arise from the T-O stretching in different tetrahedral units characterised by a variable number of bridging oxygens (from 0 to 4). Importantly, the spectral features of this second region are influenced by the iron oxidation state of the glass, the $Fe^{3+}/Fe_{tot.}$ ratio. Mercier *et al.* [11] were the first showing systematically Raman spectra of SiO_2-poor FeO-rich glasses (basalt) characterised by different $Fe^{3+}/Fe_{tot.}$ ratios as shown in Fig. 6B and, Di Muro *et al.* [26] expanded the Raman spectra database to reduced and oxidized SiO_2-rich FeO-rich glasses (peralkaline rhyolites, Fig. 6C). Over the few last years, the presence of iron-bearing nanocrystals has also become increasingly documented in both experimental and natural volcanic glasses [27, 28]. Although these small particles usually cannot be detected with standard optical and analytical micro-techniques such as scanning electron microscopy (SEM), they strongly affect the Raman features of glasses between 670 and 690 cm^{-1} as shown in Fig. 7 [27, 29].

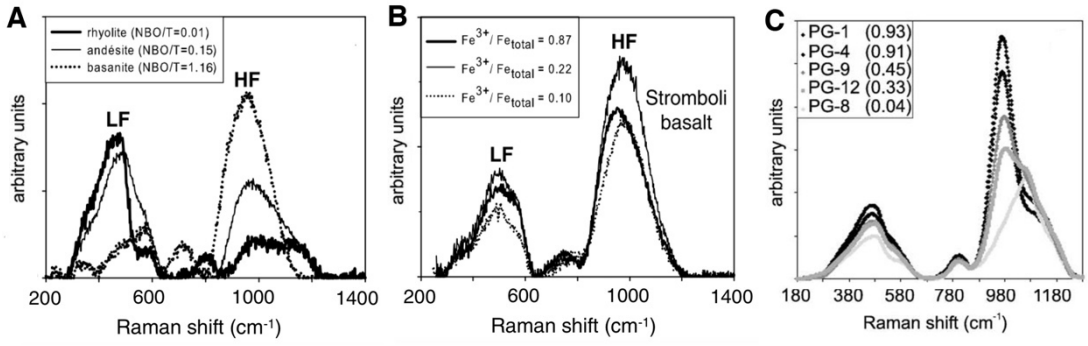

Figure 6. This shows the wide range of silicate structural envelopes. A illustrates the effect of changing the silica content (or polymerisation expressed as NBO/T). In B a relatively high-Fe basalt is shown for different Fe^{3+}/Fe total ratios and in C, low-Fe pantellerites show an even more startling change with Fe^{3+}/Fe ratios (numbers in brackets). All anhydrous samples; A and B from [11], C from [26].

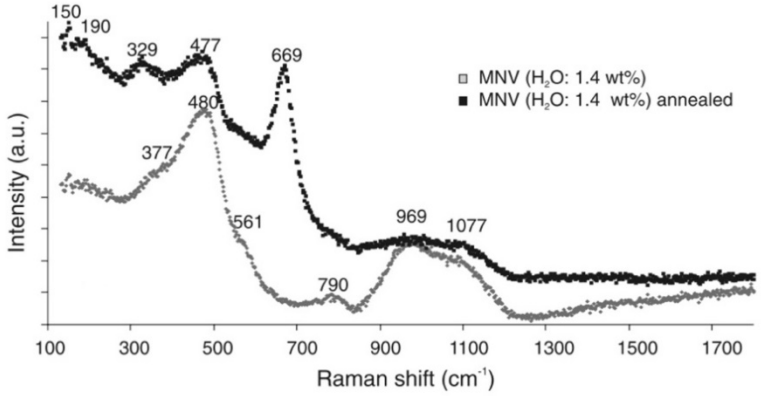

Figure 7. Change in the Raman spectrum of hydrous trachyte glasses during heating. There is a very clear appearance of sharp peaks related to iron oxide crystallisation (nanoparticles) during thermal annealing, with a concomitant decrease of the ~960 cm^{-1} band which suggest some loss of tetrahedrally coordinated Fe^{3+}in the glass structure. These changes were not seen in dry glasses annealed in the same way. Adapted from [29].

3.2. The excitation volume; heating and depth of focus

When acquiring Raman spectra, one must consider that the excitation source (laser) may locally heat up the probed sample volume and consequently oxidise the iron dissolved in the glass as shown in Fig. 7. Numerous of studies have addressed this issue (e.g., [10, 11, 27, 30]). Although sample oxidation depends on the glass composition (mainly iron, alkali and water content), and acquisition conditions (e.g., laser power, acquisition time, grating, objective), it has been demonstrated that, for confocal systems equipped with a green laser and 100x objective, ~5 mW of laser power on the sample surface and ~1 min of acquisition time are optimal conditions to limit damage to the sample

during spectra acquisition [27]. However, it is advisable to run several measurements on the same spot to identify the acquisition conditions that produce no change in the Raman spectra, in particular at ~970 cm^{-1} as shown in Fig. 7 (see [27] for further details).

In line with the potential sample alteration due to the incident light, the glass absorptivity is another factor that needs to be considered when acquiring Raman spectra of glasses. The confocal system allows for the acquisition of spectra from the sample surface to some depth and thus several studies have carefully addressed the (relative) variation of the intensity of Raman bands (i.e., silicate and water regions) with varying the depth of focus (e.g., [10, 11, 31]). The depth at which Raman spectra are acquired plays a crucial role in the choice of the methodology used to estimate the water content [31]. Based on observations from several studies of volcanic glasses [10, 31], it appears that acquiring Raman spectra at 5 µm below the sample surface is optimal. A detailed discussion on the effect of chemical composition, focus depth and confocality settings on the water estimation reliability is extensively reported in Schiavi *et al.* [31].

3.3. Baseline corrections

Several studies have discussed best procedures for treating Raman spectra of both synthetic and natural glasses when estimating the water content dissolved [9-12, 21, 22, 27, 30-32]. Recent studies (e.g., [10, 11, 26]), now seem to have come to a general agreement that the baseline correction can be greatly improved by first correcting Raman spectra for the effects of temperature and elastic scattering of the excitation source [33], as if follows:

$$I = I_{obs} \cdot \left\{ \nu_0^3 \cdot \nu \frac{[1-\exp(-hc\nu/kT)]}{(\nu_0-\nu)^4} \right\} \quad (1)$$

where I_{obs} is the Raman spectra intensity, v_0 is the wavenumber of the incident laser light (10^7/532 cm^{-1} for the green laser), v is the measured wavenumber in cm^{-1}, h is the Planck constant (6.62607×10^{-34} J s), c is the speed of light (2.9979×10^{10} cm s^{-1}), k is the Boltzmann constant (1.38065×10^{-23} J K^{-1}), and T the absolute temperature. It should also be noted that the Long-correction allows for comparisons of spectra collected with different laser and at different temperature (see Neuville *et al.* [34] and references therein).

After applying such a correction, the choice of the baseline needs to be carefully addressed. Currently, there is no universal procedure to follow for the baseline fitting and subtraction as illustrated by the examples in Fig. 8 and demonstrated by the number of studies published discussing different approaches (e.g., [9-12, 21, 22, 27, 30-32]).

The different approaches proposed rely on the use of 1) multi-linear function interpolating minima (e.g., [31]); 2) a cubic spline function [10, 12]; or 3) a 3rd order polynomial function (e.g., [26, 27, 31]). It must be noted that both the first and second approach (excluding Behrens *et al.* [10]) require knowledge of the sample composition to some extent. On the other hand, the latter is composition

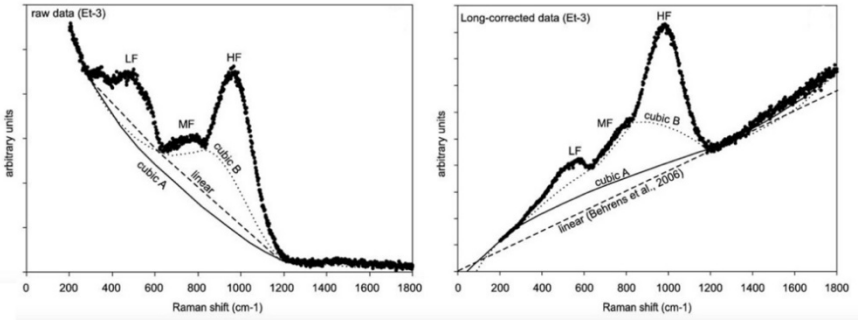

Figure 8. Various baseline fitting procedures for raw and Long-corrected spectra. Note the addition of a medium frequency envelope (MF) in this sample. From [26].

independent. These approaches result in substantial differences in the spectral feature of the silicate region, while it returns a similar feature in the water region. Le Losq *et al.* [12] and Schiavi *et al.* [31] provided a detailed discussion of the different approaches and their applicability.

3.4. Determining the water content

Here we outline the two main approaches used in the literature for retrieving the water content dissolved in glasses; the so-called external and internal calibrations. As previously stated, Raman spectroscopy is not intrinsically a quantitative method not least because the volume excited by the laser varies in an unknown way. Therefore, spectra treatment and calibration procedures need to be established *a priori* and used for both standards and samples. The choice of calibration to be used can depend on the silicate system analysed (e.g., iron-free versus iron-bearing) and/or on standards availability. However, we stress that the use of the calibration is essentially arbitrary and, as long as the procedure is consistent among all samples investigated, and the effect of the iron is considered, the choice does not have a relevant effect on the water estimation.

3.4.1. External calibration. After Long- and baseline correction, one can calculate the integrated intensity (i.e., area) of the O-H stretching vibration (i.e., water band). In a study of synthetic and multicomponent glasses, Behrens *et al.* [10] demonstrated a (chemical dependent) linear relationship between the water content and the area of the water band. Recently, Di Genova *et al.* [27] and Schiavi *et al.* [31] have demonstrated a single and linear relationship between the content and the area of the O-H stretching vibrations area for a range of volcanic glasses. They suggest that the water content dissolved in the glass can be estimated by comparison with standards that do not have to necessarily match that of the investigated sample composition. Importantly, Di Genova *et al.* [27] tested the effect of sample oxidation and magnetite nanolites on the reliability of the procedure, while Schiavi *et al.* [31] provided a detailed discussion of the best instrumental configuration.

3.4.2. Internal calibration. This procedure relies on the ratio of the integrated intensity of the water region (A_w) over the silicate area (A_s). Given that the bulk sample chemistry and,

importantly, the iron oxidation state define the spectral feature in the silicate region, this procedure depends on the sample composition. Behrens *et al.* [10] showed that this calibration is composition dependent, although Le Losq *et al.* [12] provided a more sophisticated strategy to incorporate chemical effects into the baseline procedure. They demonstrated that the A_w/A_s ratio linearly correlates with the water content of the sample regardless of the sample chemistry. Recently, it has been reported [27, 31] that for iron-rich samples (e.g., basanite and pantellerite) a further correction may be required in order to obtain a single calibration.

3.5. Water calibration for ATR

One advantage or ATR is the apparent lack of highly composition dependant extinction coefficients or the need to measure the sample thickness, which are required by transmission methods. However, some calibration is still required and has been extensively investigated by Lowenstern and Pitcher [14] for a range of geological compositions.

We continue to extend the compositional range with new data presented in Fig. 9. This appears to substantiate the generic formula of Lowenstern and Pitcher [14]

$$\text{Wt\% } H_2O = (550*A_{3450}/\text{density}) - 0.19$$

where A_{3450} is the absorbance at 3,450 cm^{-1} and the density is in g/cm^3 (see Fig. 10).

The density can usually be calculated, but ideally the conditions of formation should be known (at the glass transition) or the sample measured if sufficient material is available.

The greater wavenumber range shown for the phonotephrites in Fig. 9 illustrates the molecular water peak at 1,630 cm^{-1} (also see Fig. 2A) as well as the asymmetric stretch bands for carbonate around 1,415 cm^{-1}. Quantification for CO_2 using this carbonate peak explored further in section 3.6.

3.6. CO_2 calibration for ATR

As seen in Fig. 9, the asymmetric stretching peaks of carbonate as seen around 1,415 cm^{-1}. In Fig. 11 we show preliminary data for quantification using this peak. As can be seen in Fig. 11A, the doublet is somewhat variable with the two peaks usually the same height, but either can become dominate. As a result, the area is a more useful way to explore the concentration relationship. It is clear from Fig. 11A that the area is not linearly scaled to the known concentrations in these particular sample as shown further in Fig. 11B. Although a significant compositional range is covered in this dataset, the outliers (in blue) from the main trend do not have any obvious composition features that would group them together. Although the calculated density at 1 bar also do not appear anomalous, these samples were quenched from pressurized experiments at

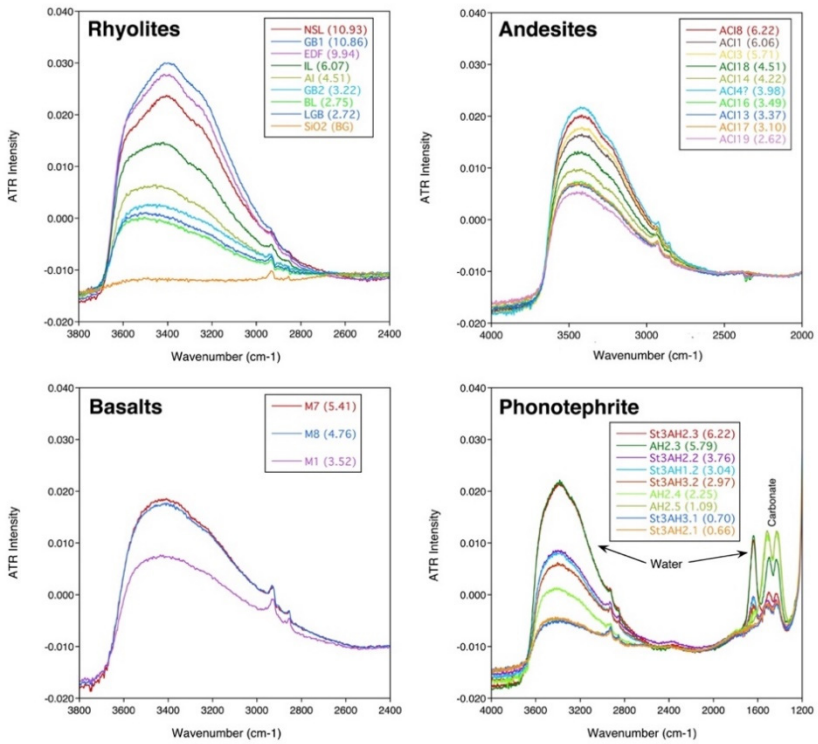

Figure 9. ATR spectra for various experimental glasses with known water contents (measure by Karl Fisher Titration and given in brackets). Rhyolites cover a range of compositions (including a very dry SiO_2 background 'blank'), but other data sets are for a fixed composition made and constant pressure and temperature (all supplied by the Hannover group). The phonotephrite samples also have varying amounts of CO_2 added. The 'St' samples have 0.32 - 0.43 wt%, AH2.3 has 0.8 wt%, and AH2.4 and AH2.5 have 0.9 wt % added CO_2.

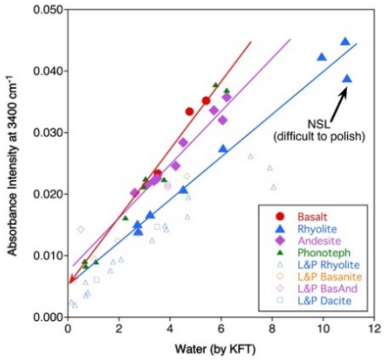

Figure 10. This shows the raw intensities from Fig. 9 plotted against the water contents. Also shown are the data from Lowenstern and Pitcher [14] which is calibrated by transmission IR and /or manometry. The raw data from this study run parallel to the L&P trends and subtraction of the background (SiO_2) would align the datasets. As shown in Lowenstern and Pitcher [14] a correction for the density or refractive index would tend to bring all the data onto a common fit.

0.2 - 0.5 GPa compared to 1.5 GPa for all other samples, and this appears to be the distinguishing feature. It is assumed this related to the density of the glass (which affects the 'path length') as shown for water in the Lowerstern and Pitcher [14] calibration.

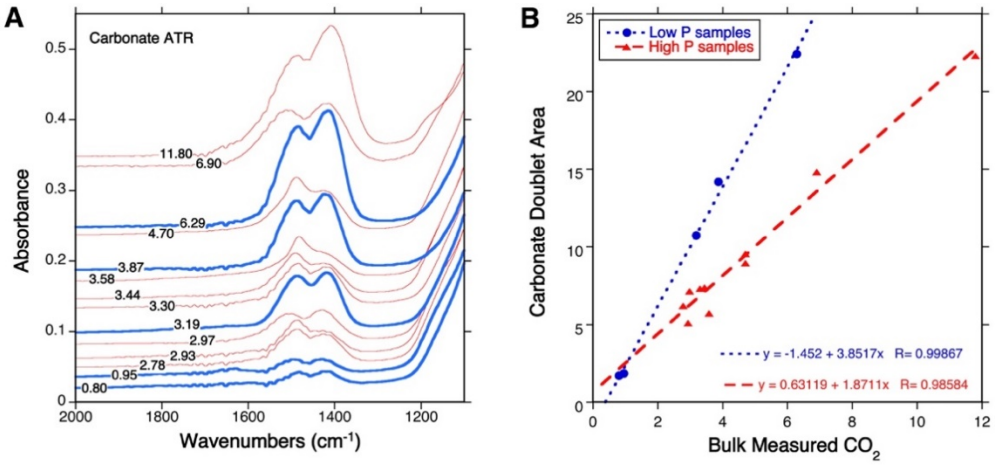

Figure 11. ART absorbances for a series of glasses with increasing CO_2 contents measured by LECO bulk C&S analyser. Most were prepared at 1.5 GPa [17] with a subset prepared at 0.2 - 0.5 GPa [35]. The wt% values are shown next to each spectrum in A. Note the relatively large absorbance for the blue spectra (lower pressure samples) which is also illustrated in B.

4. CONCLUSION

Recent advances bring us ever closer to reliable estimates of water and CO_2 content via these relatively new 'one-sided' analytical techniques. We have a better understanding of the silicate part of the Raman spectra which is essential for volatile quantification. ATR of more standards continues to improve this technique.

5. REFERENCES

[1] King P L and Larsen J F 2013 *Amer. Mineralogist* **98** 1162-1171
[2] Newman S, Stolper E M and Epstein S 1986 *Amer. Mineralogist* **71** 1527-1541
[3] Fine G and Stolper E 1985 *Contrib. Mineral. Petrol.* **91** 105-121
[4] Fine G and Stolper E 1986 *Earth Planet. Sci. Lett.* **76** 263-278
[5] Stolper E, *et al.* 1987 *Amer. Mineralogist* **72** 1071-1085
[6] Hauri E, *et al.* 2002 *Chem. Geol.* **183** 99-114
[7] Blundy J, *et al.* 2008 in: *A volcano rekindled: The renewed eruption of Mount St. Helens, 2004-2006*. (Sherrod D R, Scott W E and Stauffer P H; Eds.) US Geol. Surv. Prof. Paper 1750 755-790
[8] Brooker R A, *et al.* 2011 *Bull. Volcanol.* **73** 959-981

[9] Thomas R 2000 *Amer. Mineralogist* **85** 868-872
[10] Behrens H, *et al.* 2006 *Chem. Geol.* **229** 96-112
[11] Mercier M, *et al.* 2009 *Geochim. Cosmochim. Acta* **73** 197-217
[12] Le Losq C, *et al.* 2012 *Amer. Mineralogist* **97** 779-790
[13] Morizet Y, *et al.* 2013 *Amer. Mineralogist* **98** 1788-1802
[14] Lowenstern J B and Pitcher B W 2013 *Amer. Mineralogist* **98** 1660-1668
[15] McMillan P F and Hess A C 1988 *Rev. Mineralogy* **18** 11-62
[16] Brooker R A, *et al.* 1999 *Geochim. Cosmochim. Acta* **63** 3549-3565
[17] Brooker R A, *et al.* 2001 *Chem. Geol.* **174** 241-254
[18] Dixon J E, *et al.* 1995 *J. Petrology* **36** 1607-1631
[19] Brooker R A, *et al.* 2001 *Chem. Geol.* **174** 225-240
[20] Mysen B O and Virgo D 1986 *Chem. Geol.* **57** 303-331
[21] Chabiron A, *et al.* 2004 *Contrib. Mineral. Petrol.* **146** 485-492
[22] Zajacz Z, *et al.* 2005 *Contrib. Mineral. Petrol.* **150** 631-642
[23] McMillan P and Piriou B 1982 *J. Non-Crystalline Solids* **53** 279-298
[24] Mysen B O 1988 *Structure and properties of silicate melts*. (Amsterdam, the Netherlands: Elsevier) pp. 354
[25] Seifert F, *et al.* 1982 *Amer. Mineralogist* **67** 696-717
[26] Di Muro A, *et al.* 2009 *Chem. Geol.* **259** 78-88
[27] Di Genova D, *et al.* 2017 *Chem. Geol.* **475** 76-86
[28] Mujin M, *et al.* 2017 *Amer. Mineralogist* **102** 2367-2380
[29] Di Muro A, *et al.* 2006 *Appl. Geochem.* **21** 802-812
[30] Thomas R, *et al.* 2008 *Zeitschrift. geol. Wissenschaften* **36** 31-37
[31] Schiavi F, *et al.* 2018 *Chem. Geol.* **483** 312-331
[32] Di Muro A, *et al.* 2006 *Geochim. Cosmochim. Acta* **70** 2868-2884
[33] Long D A 1977 *Raman spectroscopy*. (New York, NY: McGraw-Hill) pp. 276
[34] Neuville D R, *et al.* 2014 *Rev. Mineralogy* **78** 509-541
[35] Brooker R A and Kjarsgaard 2011 *J. Petrology* **52** 1281-1305